The Influence of the Opening Size on the Shear Performance of the Cross-laminated Timber (CLT) Walls

Daiyuan Zhang,[a] Liming Shen,[a,*] Xudong Zhu,[b] Sujun Zhang,[b] and Meng Gong [c]

Cross-laminated timber is a wood product with excellent fire resistance and mechanical performance that is often used in tiny houses. Using the ASTM standard E564, the shear performance of cross-laminated timber wall panels, with and without openings, were investigated in this study. The specimens were made of spruce-pine-fir II_c lumber and installed on a test platform using high-strength bolts passing through them. This connection mode limited the displacements obtained in the test, primarily the shear displacements and rocking displacements. By comparing the static load test data of the three specimens with openings and the one without an opening, it was found that openings reduced the shear strength and shear stiffness. For the same sized rectangular opening, the shear stiffness of the cross-laminated timber panel was less when the wider side was horizontal (normal to the direction of the applied force). The shear stiffness of the cross-laminated timber wall panels can be effectively improved by reinforcing the areas near the openings with metal sheets. With reinforcement, the shear strength did not change drastically, but the damage to the cross-laminated timber wall panels was significantly reduced.

Contact information: a: College of Science and Engineering, Nanjing Forestry University, Nanjing 210037 China; b: Yangzhou Polytechnic Institute, Jiangsu 225200 China; c: Wood Science and Technology Centre, University of New Brunswick, 1350 Regent St, Fredericton E3C 2G6 Canada;
* Corresponding author: shenlimingda@hotmail.com

INTRODUCTION

Cross-laminated timber (CLT), a wood product intended for construction, was developed in Germany and Austria in the 1980s, and has been widely adopted around the world. Since 2000, CLT has been extensively used for residential and nonresidential applications in Europe. The European production of CLT increased from 25000 m^3 in 1996 to 340,000 m^3 in 2010 (Gagnon and Pirvu 2011). Outside of Europe, *e.g.*, in Canada and Australia, CLT has also experienced rapid growth as a new type of construction material. A CLT wall has several structural advantages over a traditional light-frame wood-joisted wall, including bidirectional strength and stiffness, fire resistance, and dimensional stability (Frangi *et al.* 2008, 2009; Klippel *et al.* 2014; Brandner *et al.* 2015; Wang *et al.* 2015; Sikora *et al.* 2016). In addition, in seismically active regions, CLT structures have shown good seismic resistance (Gavrić *et al.* 2012; Hristovski *et al.* 2013; Izzi *et al.* 2018; Hashemi and Quenneville 2020). Cross-laminated timber constructions also reduce carbon emissions. A study by Hammond and Jones (2008) found that a six-story CLT building contributes 724 tons of carbon dioxide to the atmosphere annually, while a reinforced concrete building of the same volume contributes 1984 tons of carbon dioxide.

A tiny house is generally defined as a house with an area no greater than 37 m^2. It is usually a wooden structure or container structure, with wooden structures being more popular. Tiny houses reflect a movement to small houses in the United States at the end of the 20th century. This movement rapidly developed in North America after the financial crisis in 2008, and tiny houses have become popular in Europe and Oceania as well. Wooden tiny houses are widely used to provide housing for low-income people, to meet the need for post-disaster reconstruction, and for temporary camps and scenic resort hotels. Tiny houses used for post-disaster reconstruction, as well as those used in harsh natural conditions, need to have good wind, earthquake, and corrosion resistance. They also need to be low cost and suitable for rapid construction. As such, CLT tiny houses made of spruce-pine-fir (SPF) lumber may meet these needs (Yeh *et al.* 2012).

The wind resistance and seismic performance of a CLT wall system is primarily related to its behavior when subjected to lateral loads (Zhou *et al.* 2014). Other researchers have conducted experimental studies on the performance of CLT walls under both static and cyclic lateral loads (Reynolds *et al.* 2017; Li *et al.* 2020). The kinematic behavior of CLT wall systems under lateral loads is different from that of traditional light-frame wooden walls (Gavric *et al.* 2015; Crovella *et al.* 2019). It has been demonstrated that CLT walls have higher in-plane stiffness when compared to traditional light-frame walls. Most of the deformation due to lateral loads is concentrated at the anchoring connections and at the screwed vertical joints between adjacent CLT wall panels (Gavrić *et al.* 2014).

Openings in a wall for windows and doors have a considerable effect on the shear performance of the wall. The load-bearing capacity and stiffness of wood walls with openings are primarily influenced by the size and layout of the openings. In the past, wood-frame buildings were designed for earthquake and wind loads by considering the shear resistance of full wall segments only (Dujič *et al.* 2009). However, for a wood-frame tiny house, the walls are so small that the openings must be considered in the evaluation of strength and stiffness. In this study, tiny-house CLT walls were prepared using SPF II$_c$ lumbers, and the influence of the size of the openings on the shear performance of the CLT walls was studied. Recently, some Italian researchers investigated the kinematic modes of CLT shear-walls with openings; the results show a decreasing tendency of the degree of coupling with increased lintel beam slenderness (Mestar *et al.* 2020).

EXPERIMENTAL

Materials

The SPF lumber used in this study was bought from Suzhou Jingxiu Construction Technology Co. Ltd. (Suzhou, P. R. China). It is a broad-grained wood, and the share of latewood is 25.3%. The average density of the timber is 0.45 g/cm^3, and it was air-dried to an average moisture content of 9.41% at room temperature and humidity (23 °C and a relative humidity of 65%). The SPF boards, 4000 mm in length (L), 89 mm in width (W), and 38 mm in thickness (T), were fabricated into 800 mm x 80 mm x 16 mm standard wood strips. The strips were then assembled *via* a cold press machine, and resin with a yield of 200 g/m^2 was added between the layers. The adhesive was one component polyurethane (PUR) (PURBOND HB S709). This is a common thermosetting one component PUR adhesive. The pressure of the cold press was held steady at 20 MPa for 8 h to 12 h at a temperature of 15 °C. Afterwards, 1200 mm x 1200 mm x 48 mm three-layer CLT panels were obtained and were trimmed into 1100 mm x 1100 mm x 48 mm CLT wall specimens.

The fabrication processes of the specimens are shown as Fig. 1, and the dimensions of the openings for all three kinds of CLT walls are listed in Table 1.
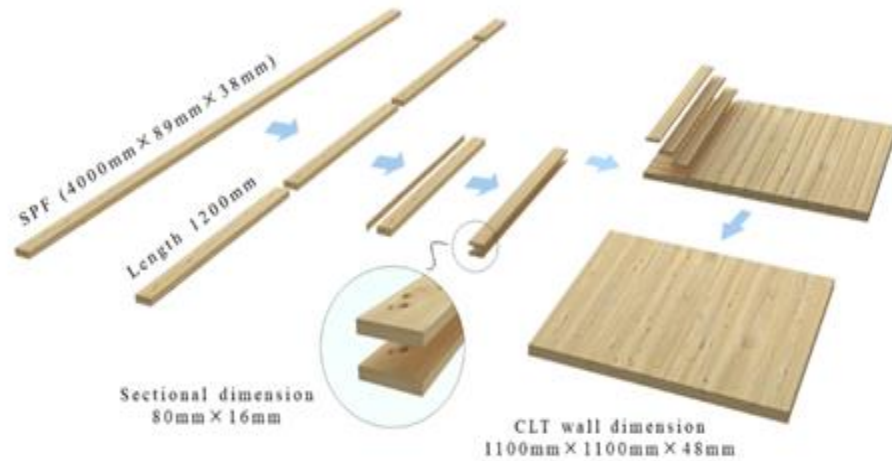
Fig. 1. Fabrication processes of the CLT walls

**Table 1.** The Dimensions of CLT Wall-specimen Openings

Number	Opening Dimension (Width × Height) (mm)	Specimen Sketch
FW	-	
OW-1	500 x 500	

OW-2	600 x 500	
OW-3	500 x 600	

Figure 2 shows all the metal connectors and fasteners used in this study. The CLT wall specimens were fixed to an underlying steel beam using eight custom angle brackets and two kinds of bolts.

Fig. 2. The metal connectors and fasteners used in the CLT wall tests
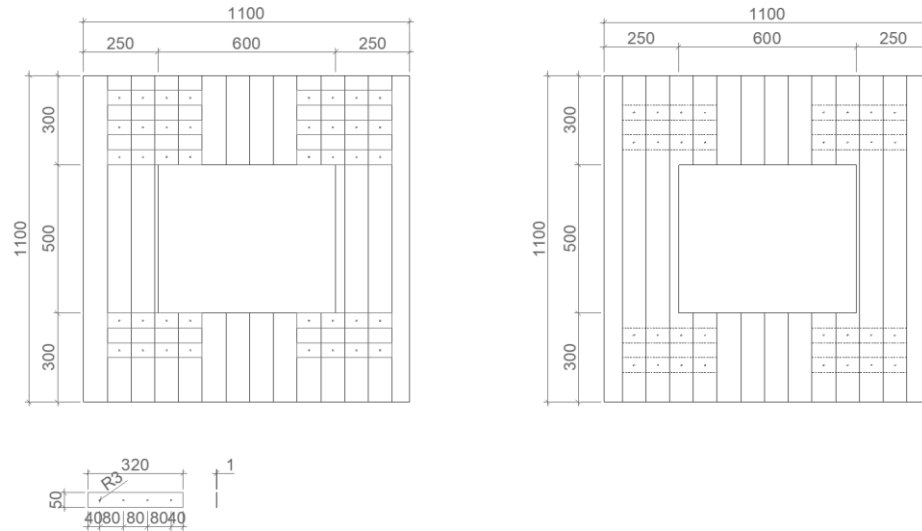
Fig. 3. Reinforcement on both sides of the OW-2 specimen (the left diagram shows the front side)

The CLT wall specimens were connected with angle brackets by eight 8.8 grade high-strength bolts with a diameter of 10 mm and a length of 100 mm. The connection between the angle bracket and the underlying steel beam were fixed by sixteen 8.8 grade high-strength bolts with a diameter of 20 mm and a length of 60 mm. In this study, a 320 mm (L) × 40 mm (W) × 1 mm (T) steel plate was selected to reinforce the wall opening area. A 4 mm diameter self-tapping screw (STS) was used to fix the steel plate to the CLT wall specimens (Pai 2014). The reinforcement position is shown in Fig. 3; ten steel plates on the front side and eight on the back side of the CLT wall.

Test Equipment

The tests were carried out at the mechanics laboratory of the Yangzhou Institute of Industry and Technology (Yangzhou, China). The horizontal static loading test was carried out using a YD-IID testing machine developed by Yantai Measurement and Control Technology Co. Ltd (Shandong, China). The maximum loading force of the horizontal load was 300 kN, and the maximum displacement was 200 mm. As shown in Fig. 4, there was a distribution steel beam at the top of the CLT shear wall. A vertical load of 5.5 kN was applied to the top of this steel beam. A 5G10X series displacement meter (Jiangsu Donghua Testing Technology Co. Ltd, Taizhou, China) was selected to detect the horizontal displacement at the top of the CLT walls. The displacement and load data were collected using a DH3816N test system produced by the same company, with a collection frequency of 1 Hz.

Methods

The static loading test was carried out in accordance with ASTM standard E564-06 (2018), and its displacement rate was 0.2 mm/s. Multiple rounds of loading were applied in accordance with the estimated ultimate loads of 10%, 30%, and 60%. Each time, the load was held for 5 min, then removed, and another 5 min was waited. Then, the next higher load level above the backoff load was applied, and the process was continued until the ultimate load was reached (ASTM E564-06 2018).

The shear stiffness and shear strength of the CLT wall was calculated according to the lateral load, the horizontal displacement at the top of the CLT wall, and the diagonal dimension change (δ) obtained from the test.
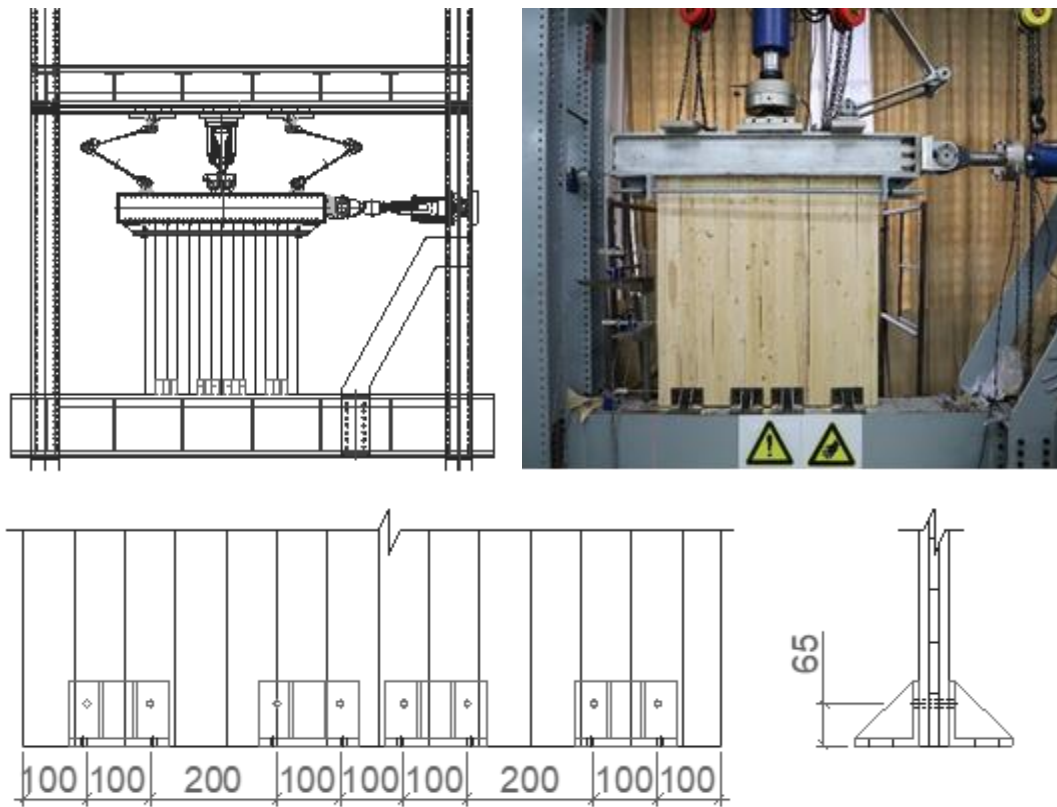

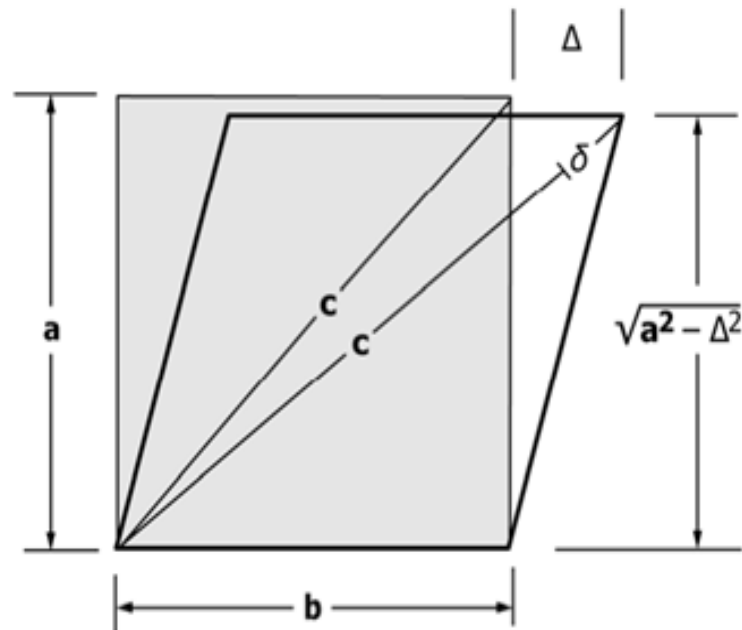**Fig. 4.** Experimental setup for the static load tests

Fig. 5. Horizontal measurement (ASTM E564-06 2018)

The formula for global shear stiffness G' was taken from ASTM standard E564-06 (2018), as shown in Eq. 1,

$$G' = \frac{P}{\Delta} \times \frac{a}{b} \tag{1}$$

where G' is the global shear stiffness, kN·m^{-1}, P is the load, kN, Δ is the total horizontal displacement of the top of the wall, mm, a is the height of the CLT shear wall, mm, and b is the length of the CLT shear wall, mm.

The formula for the internal shear stiffness (G_{int}) was adopted from ASTM standard E564-06(2018), as shown in Eqs. 2 and 3,

$$G_{int} = \frac{P}{\Delta_{int}} \times \frac{a}{b} \tag{2}$$

$$\Delta_{int} = \frac{(2C\delta + \delta^2)}{2b} \tag{3}$$

where G_{int} is the internal shear stiffness (kN·m^{-1}), P is the load, Δ_{int} is the internal horizontal displacement of the top of the wall (mm), C is the initial length of the diagonal of the CLT wall, mm, and δ is the diagonal elongation (mm). The formula for ultimate shear strength (S_u), kN·m^{-1}, according to ASTM standard E564-06 (2018), is shown in Eq. 4,

$$S_u = \frac{P_u}{b} \tag{4}$$

where Pu is the highest load level held long enough to record gauge measurements (kN).

The yield strength (P_y), kN, of the CLT walls was calculated based on the load displacement curve of the wall and the calculation method (Dong *et al.* 2015). That calculation method is as follows: Connect points 0.1 P_{max} and 0.4 P_{max} to form line I. Then connect 0.4 P_{max} and 0.9 P_{max} to form line II. Next, translate line II to be tangent to the curve and call this tangent line III. The horizontal line at the intersection of the tangent line III and line I is line IV, and its ordinate value is the yield load P_y.
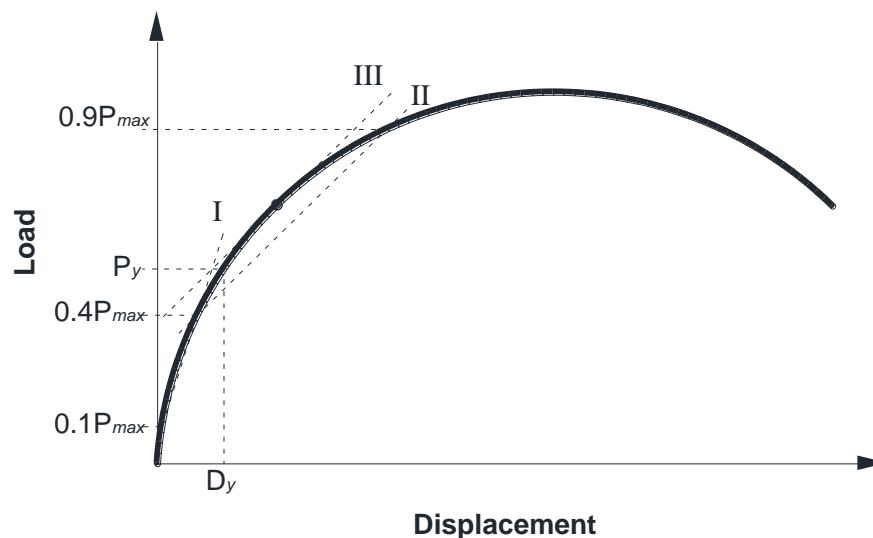

Fig. 6. Analysis method of the characteristic value

RESULTS AND DISCUSSION

Mechanical Properties

According to the research of Gavric *et al.* (2012), the total displacement (δ_{tot}) of a CLT wall is the sum of four components, *i.e.*, the rocking (δ_r) (Fig. 7 a), sliding (δ_{sl}), shear (δ_{sh}) (Fig. b), and bending (δ_b) deformations. Based on numerous CLT wall tests performed in the past, the most important deformation components are rocking and sliding, whereas shear and bending distortions of the CLT wall are considerably less important (Popovski *et al.* 2010; Ceccotti *et al.* 2013; Seim *et al.* 2013; Tomasi 2013). This is because most tests used hold-downs and nails to connect the CLT walls and the test setup. Thus, the pure shear failure of nails was usually the primary form of damage, so nearly all deformation of the CLT walls was sliding.

In this study, the 10 mm diameter high-strength bolts used to connect the CLT walls to the angle brackets passed through the panels, limiting the sliding displacement of the CLT wall. Thus, the deflection of the CLT walls in this study consisted primarily of rocking and shear, as shown in Fig.7 (c). Due to the fact that both the height and width of the CLT wall specimen were 1100 mm, the upside displacement of the specimen U_y in Fig. 7 was equal to δ_r. Figure 8 shows the load-displacement curves of the full-size CLT wall specimens as well as the specimens with three kinds of openings. Combined with the test data shown in Table 2, these results show that the failure load of the FW specimen (the one with no openings) was 96.6 kN, and the corresponding S_u was 87.8 kN·m^{-1}. The effect of openings on the shear strength of the CLT wall is obvious. The ultimate shear strength of the opening wall-1 (OW-1) specimen with an opening size of 500 mm x 500 mm was 69.9 kN·m^{-1}, which is 20.39% less than the ultimate shear strength for the FW specimen. According to the S_u values of the opening wall-2 (OW-2) and opening wall-3 (OW-3) specimens, it was found that an increase in the height of the opening had a greater impact on the strength than an increase in its width.
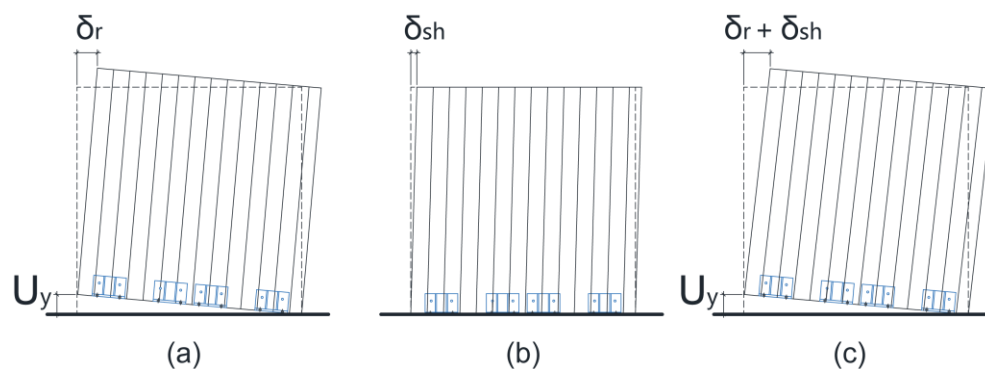

Fig. 7. Deflection components of a single CLT wall panel: (a) rocking; (b) shear; (c) total deflection in the test

By observing the four load-displacement curves of the CLT wall specimens, it was found that the stiffness of the OW-2 specimen was considerably less than the stiffness of the other CLT wall specimens. The global shear stiffness and internal shear stiffness data confirmed this conclusion. Figure 8 shows the global stiffness and internal shear stiffness of the FW specimen (without an opening) as well as the three specimens with openings. Since the global stiffness is greatly affected by the rocking displacement, the internal stiffness is more representative of the stiffness of the CLT walls. As can be seen in Fig. 9,

the stiffness of all specimens with openings was considerably less than the stiffness of the FW specimen, *i.e.*, the one without openings. The internal stiffness of the OW-2 specimen was the least, 4881 kN·m^{-1}, which was only 57.1% of the internal stiffness of the FW specimen.

Table 2. Mechanical Properties of the CLT Wall Specimens (OW-2R is Defined in Materials)

|	δ_r (mm)	δ_{sh} (mm)	Δ (mm)	δ (mm)	P (kN)	P_y (kN)	G' (kN·m^{-1})	G_{int} (kN·m^{-1})	S_u (kN·m^{-1})
FW	10.0	11.8	21.8	8.0	96.6	81.2	7595.2	8547.3	87.8
OW-1	6.0	11.8	17.8	10.0	76.9	-	4960.8	5439.9	69.9
OW-2	7.0	13.0	20.0	15.0	69.0	51.0	4509.8	4881.0	62.7
OW-3	4.0	10.1	14.1	9.0	65.2	-	5155.6	5126.3	59.3
OW-2R	2.0	12.8	14.8	5.0	69.7	43.7	6764.7	9877.0	63.4
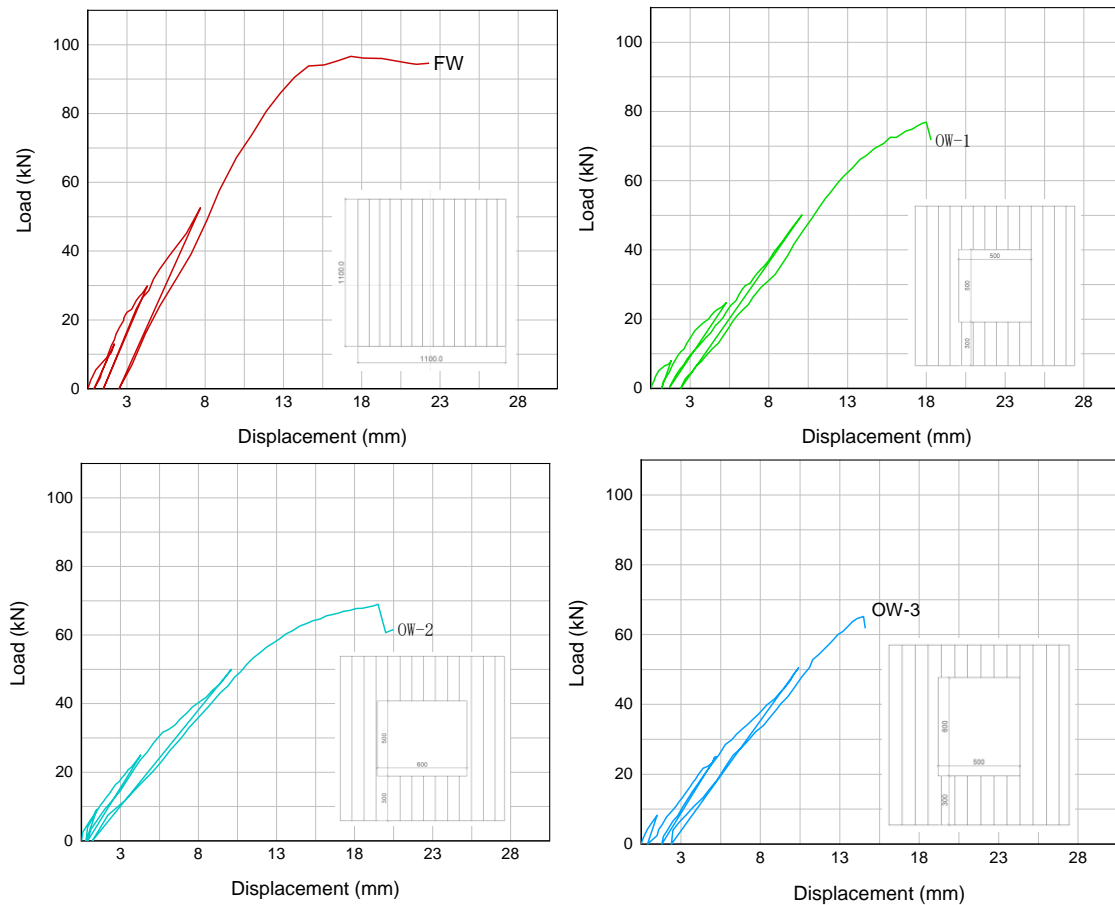
Fig. 8. Load-displacement curves of CLT wall specimens

Figure 10 shows the percentages of the rocking displacement (δ_r) and shear displacement (δ_{sh}) in terms of the total displacement (δ_{tot}) of each specimen. The proportion of rocking displacement of the FW specimen was as high as 46%, which was due to the high shear strength of the complete CLT plate, and the failure of the specimen primarily was caused by the rocking displacement at the bottom joint. The shear displacement proportion of the three CLT wall specimens with openings and without reinforcement was between 65.0% and 71.6%. The failure strength of a CLT wall with an opening decreased when it was subjected to a lateral load; therefore, the wall displacement was caused primarily by shear deformation due to the limited effect of the bolts on the wall.
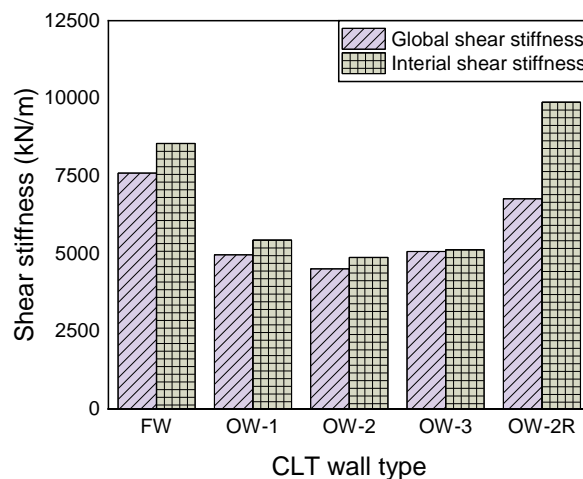

Fig. 9. Shear stiffness of the unreinforced CLT wall specimens (FW: Full Wall, OW-1: Opening Wall-1, OW-2: Opening Wall-2, OW-3: Opening Wall-3, OW-2R: Opening Wall-2 Reinforced)
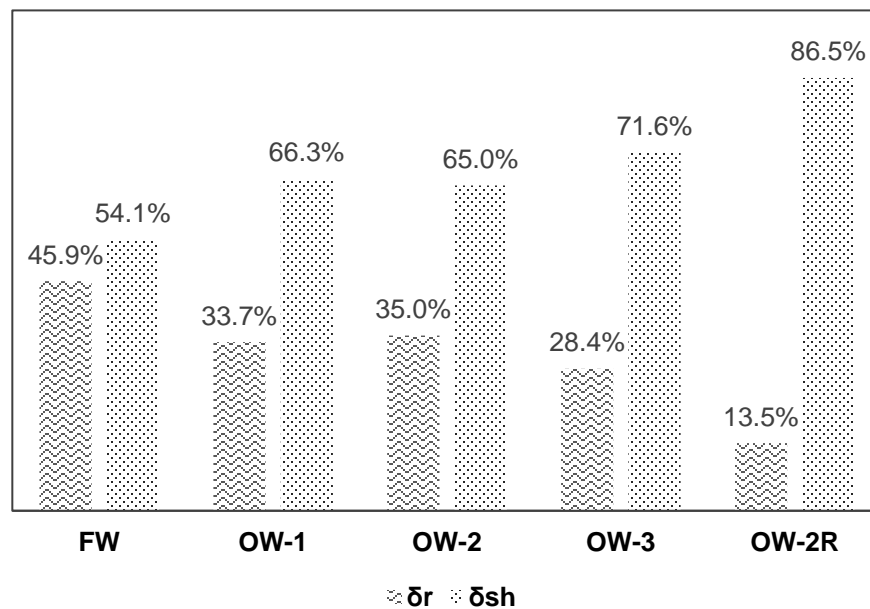
Fig. 10. The percentages of the deflection components of the CLT wall specimens

Failure Modes

Figure 11 shows the typical failure modes of the CLT walls with and without openings during the lateral static loading tests. It can be seen from Fig. 11 that the failure of the FW CLT wall specimen primarily manifested as the crushing of the lumber in the lower left corner and a shearing failure of the lumber under the bolt hole in the lower right corner. These two failures strongly indicated that more rocking displacement occurred in the FW specimen. The failure position in the OW-1 specimen occurred at the left of the lower side of the opening, and primarily manifested as the separation of the outer SPF lumber and the inner lumber. The OW-2 specimen had a larger width (600 mm) and its failure occurred at the upper right corner of the opening, which manifested as the tearing of the lumber along the grain direction. The OW-3 specimen with the larger opening height (600 mm) showed stratified failure and wood cracking in the lower left and upper right corners of the opening area. According to the failures of the CLT walls with three different openings, the upper right corner and lower left corner of the openings are areas of stress concentration. The OW-2 specimen, with a width opening of 600 mm, had the most serious damage.

(a)   **(b)**

(c)   **(d)**
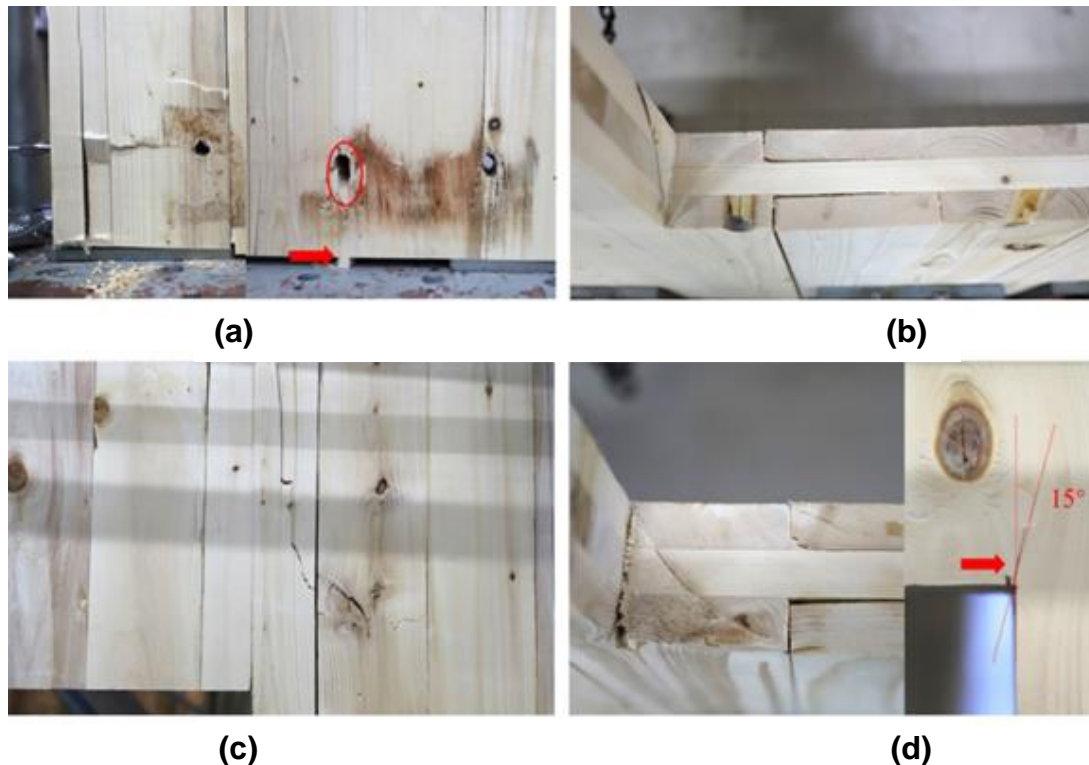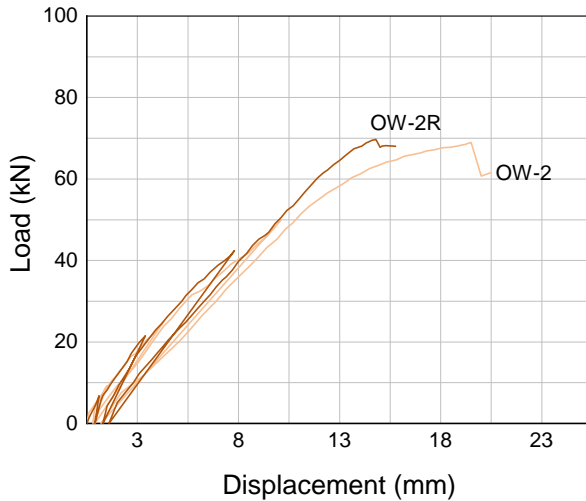
Fig. 11. Typical failure appearances of the specimens during the static load tests: (a) FW; (b) OW-1; (c) OW-2; and (d) OW-3

Reinforcement Effect of the Opening Area

Based on a comparison of the failure strength, shear stiffness, and plate failure of the specimens with openings, the OW-2 specimen was selected for reinforcement in this study; thus, the authors designed a reinforced specimen (OW-2R). Figure 12 shows the load-displacement curves of the OW-2 and OW-2R specimens. The failure load of the OW-2R was not much better than the failure load of the OW-2 specimen, but the shear stiffness was considerably better. Combining the data in Table 2 with the data in Figs. 10 and 13, it

bioresources.com

was found that the shear displacement (δ_{sh}) accounted for a large proportion of the total displacement (δ_{tot}) of the reinforced CLT wall, reaching 86.5%. The internal shear stiffness of the reinforced CLT wall OW-2R was 102.4% greater than the internal shear stiffness of the OW-2, reaching 9877 kN·m⁻¹, which was greater than the internal shear stiffness of the CLT wall without an opening. In terms of the failure modes, the failure location of the reinforced CLT wall still appeared at the upper right corner of the opening, but the size of the failure crack was far smaller than the failure crack in the OW-2 specimen (as shown in Fig. 14).

Fig. 12. Load-displacement curves of the non-reinforced OW-2 and reinforced OW-2R specimens
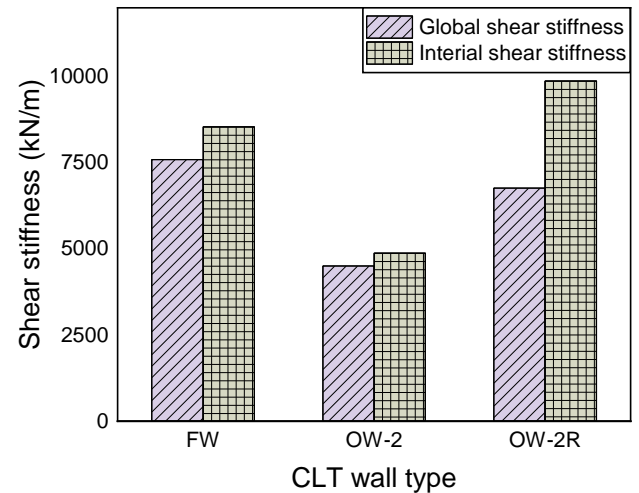
Fig. 13. Shear stiffness of the FW, OW-2, and OW-2R specimens

(a)   **(b)**
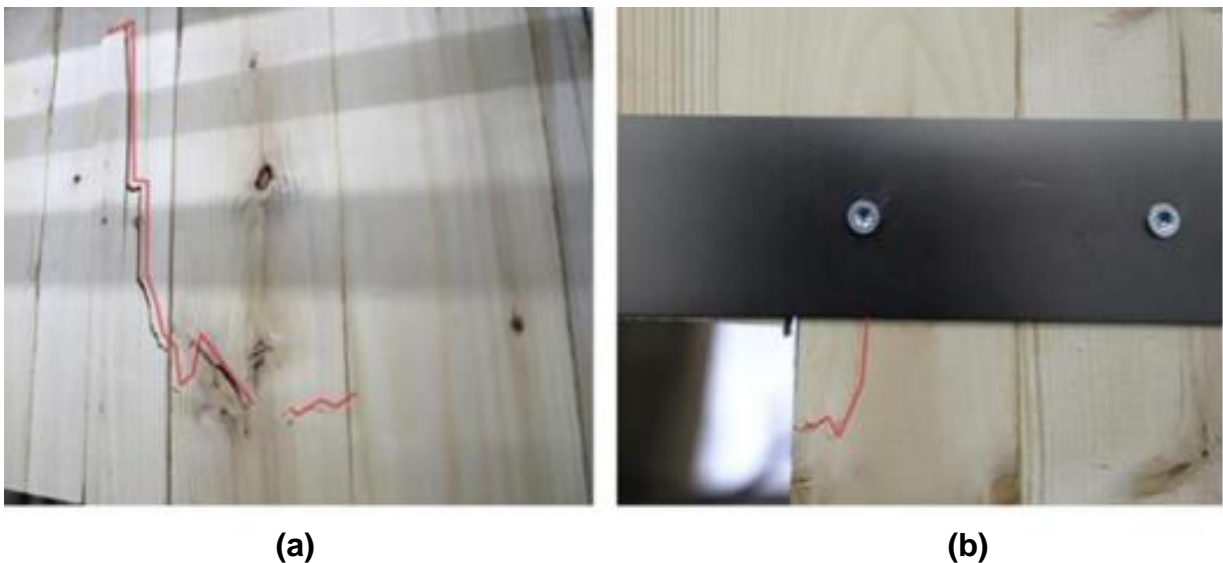
Fig. 14. Typical failure appearances of specimens during static load: (a) OW-2; and (b) OW-2R

bioresources.com

CONCLUSIONS

1. Compared with the traditional CLT wall panels connected by hold-downs and nails, the displacement of the CLT wall panels connected by button-through bolts under lateral load primarily consisted of rocking displacement and shear displacement; there was almost no sliding displacement. The shear displacement of the reinforced opening CLT wall panel reached 86.5% of the total displacement. Therefore, a shear test using a bolt-through connection can more effectively reflect the shear performance of the CLT wall panel itself.

2. Having an opening in the CLT considerably reduces its ultimate shear strength and shear stiffness; the reduction in shear stiffness is more substantial. When the size of the opening is the same, the stiffness of the wall is less for larger widths than for larger heights.

3. According to the failure positions of the CLT wall panels with openings under a lateral load during the tests, the stress concentration area was the area below the opening and the corner above the opening close to the side of the lateral load. In addition, the failure of the CLT wall panels with a larger width was more serious when the opening size was the same.

4. The ultimate shear strength of a CLT wall panel with an opening was not considerably improved by using 1 mm thin steel plates to reinforce the upper and lower areas of the opening. However, the shear stiffness of the wall was greatly increased by the plates, and the crack size of the reinforced CLT wall when damaged was much smaller with the plates than without them.

ACKNOWLEDGMENTS

REFERENCES CITED

ASTM E564-06 (2018). "Standard practice for static load test for shear resistance of framed walls for buildings," ASTM International, West Conshohocken, PA.

Brandner, R., Flatscher, G., Ringhofer, A., Schickhofer, G., and Thiel, A. (2015). "Cross laminated timber (CLT): Overview and development," *European Journal of Wood and Wood Products* 74, 331-351. DOI: 10.1007/s00107-015-0999-5

Ceccotti, A., Sandhaas, C., Okabe, M., Yasumura, M., Minowa, C., and Kawai, N. (2013). "SOFIE project – 3D shaking table test on a seven-story full-scale cross-laminated timber building[‡]," *Earthquake Engineering & Structural Dynamics* 42(13), 2003-2021. DOI: 10.1002/eqe.2309

Crovella, P., Smith, W., and Bartczak, J. (2019). "Experimental verification of shear analogy approach to predict bending stiffness for softwood and hardwood cross-

laminated timber panels," *Construction and Building Materials* 229, 1-5. DOI: 10.1016/j.conbuildmat.2019.116895

Dujič, B., Klobcar, S., and Zarnic, R. (2009). "Influence of openings on shear capacity of wooden walls," *NZ Timber Design Journal* 16(1), 5-17.

Frangi, A., Fontana, M., Hugi, E., and Jübstl, R. (2009). "Experimental analysis of cross-laminated timber panels in fire," *Fire Safety Journal* 44(8), 1078-1087. DOI: 10.1016/j.firesaf.2009.07.007

Frangi, A., Fontana, M., Knobloch, M., and Bochicchio, G. (2008). "Fire behaviour of cross-laminated solid timber panels," *Fire Safety Science* 9, 1279-1290. DOI: 10.3801/IAFSS.FSS.9-1279

Gagnon, S., and Pirvu, C. (2011). *Cross Laminated Timber (CLT) Handbook,* FPInnovations, Vancouver, Canada.

Gavrić, I., Fragiacomo, M., and Ceccotti, A. (2014). "Cyclic behavior of typical screwed connections for cross-laminated (CLT) structures," *European Journal of Wood and Wood Products* 73, 179-191. DOI: 10.1007/s00107-014-0877-6

Gavric, I., Rinaldin, G., Fragiacomo, M., Ceccotti, A., and Amadio, C. (2012). "Experimental-numerical analyses of the seismic behaviour of cross-laminated wall systems." in: *Proceedings of the 15th World Conference on Earth-quake Engineering WCEE 2012*, 24-28 September, Lisbon, Portugal.

Hammond, G. P., and Jones, C. I. (2008). "Embodied energy and carbon in construction materials," *Energy* 161(2), 87-98. DOI: 10.1680/ener.2008.161.2.87

Hashemi, A., and Quenneville, P. (2020). "Large-scale testing of low damage rocking cross laminated timber (CLT) wall panels with friction dampers," *Engineering Structures* 206, 1-12. DOI: 10.1016/j.engstruct.2020.110166

Hristovski, V., Dujic, B., Stojmanovska, M., and Mircevska, V. (2013). "Full-scale shaking-table tests of XLam panel systems and numerical verification: Specimen 1," *Journal of Structural Engineering* 139(11), 2010-2018. DOI: 10.1061/(ASCE)ST.1943-541X.0000754

Izzi, M., Casagrande, D., Bezzi, S., Pasca, D., Follesa, M., and Tomasi, R. (2018). "Seismic behaviour of cross-laminated timber structures: A state-of-the-art review," *Engineering Structures* 170, 42-52. DOI: 10.1016/j.engstruct.2018.05.060

Klippel, M., Leyder, C., Frangi, A., Fontana, M., Lam, F., and Ceccotti, A. (2014). "Fire tests on loaded cross-laminated timber wall and floor elements," *Fire Safety Science* 11, 626-639. DOI: 10.3801/IAFSS.FSS.11-626

Li, Z., Wang, X., and He, M. (2020). "Experimental and analytical investigations into lateral performance of cross-laminated timber (CLT) shear walls with different construction methods," *Journal of Earthquake Engineering* (in-press), 1-23. DOI: 10.1080/13632469.2020.1815609

Mestar, M., Doudak, G., Polastri, A., and Casagrande, D. (2020). "Investigating the kinematic modes of CLT shear-walls with openings," *Engineering Structures*. DOI: 10.1016/j.engstruct.2020.111475

Pai, S. (2014). "Force transfer around openings in CLT shear walls," *Master of Applied Science*. DOI: 10.14288/1.0165581

Popovski, M., Schneider, J., and Schweinsteiger, M. (2010). "Lateral load resistance of cross-laminated wood panels." in: *Proceedings of the 11th World Conference on Timber Engineering WCTE 2010*, 20-24 June, Trentino, Italy.

Reynolds, T., Foster, R., Bregulla, J., Chang, W.-S., Harris, R., and Ramage, M. (2017). "Lateral load resistance of cross-laminated timber shear walls," *Journal of Structural Engineering* 143(12), 1-6. DOI: 10.1061/(ASCE)ST.1943-541X.0001912

Seim, W., Hummel, J., Flatscher, G., and Schickhofer, G. (2013). "CLT Wall elements under cyclic loading - Details for anchorage and connection," in: *Proceedings of the COST Action FP1004 Conference Focus Solid Timber Solutions - European Conference on Cross Laminated Timber*, 21-21 May, Graz, Austria.

Sikora, K. S., McPolin, D. O., and Harte, A. M. (2016). "Effects of the thickness of cross-laminated timber (CLT) panels made from Irish Sitka spruce on mechanical performance in bending and shear," *Construction and Building Materials* 116, 141-150. DOI: 10.1016/j.conbuildmat.2016.04.145

Tomasi, R. (2013). "Seismic behaviour of connections for buildings in CLT," in: *Proceedings of the COST Action FP1004 Conference Focus Solid Timber Solutions - European Conference on Cross Laminated Timber*, 21-21 May, Graz, Austria.

Wang, Z., Gong, M., and Chui, Y.-H. (2015). "Mechanical properties of laminated strand lumber and hybrid cross-laminated timber," *Construction and Building Materials* 101(Part 1), 622-627. DOI: 10.1016/j.conbuildmat.2015.10.035

Yeh, B., Gagnon, S., Williamson, T., Pîrvu, C., Lum, C., and Kretschmann, D. (2012). "The North American product standard for cross-laminated timber," *Wood Design Focus* 22(2), 13-21.

Zhou, Q., Gong, M., Chui, Y., and Mohammad, M. (2014). "Measurement of rolling shear modulus and strength of cross laminated timber fabricated with black spruce," *Construction and Building Materials* 64, 379-386. DOI: 10.1016/j.conbuildmat.2014.04.039